Phonon response of $Al_xGa_{1-x}Sb/GaSb$ epitaxial layers by Fourier-transform infrared-reflectance and Raman spectroscopies

R. Ferrini, M. Galli, G. Guizzetti, and M. Patrini
INFM, Dipartimento di Fisica A. Volta, Università di Pavia, via Bassi 6, I-27100 Pavia, Italy

A. Bosacchi and S. Franchi
Istituto CNR-MASPEC, Via Chiavari 18, I-43100 Parma, Italy

R. Magnanini
INFM, Dipartimento di Fisica, Università di Parma, Viale delle Scienze, I-43100 Parma, Italy

(Received 29 May 1997)

Far-infrared reflectance and first- and second-order Raman spectra were carefully measured at room temperature on a series of $Al_xGa_{1-x}Sb$ layers epitaxially grown on GaSb (with $0.0 \leqslant x \leqslant 0.5$). For all the compositions the clean ''two-mode'' behavior of lattice vibrations was confirmed. The fit of the reflectance curves with classical dielectric functions yielded the compositional variation of the TO and LO phonon frequencies, which are in very good agreement with the Raman results, as well as the oscillator strengths and the line broadenings. The effects of cation disorder were evidenced in both the reflectance and Raman spectra. A comparison was made with previous data, which show some scattering and discrepancies, having been measured by a single technique (reflectance or Raman) on samples with different characteristics. [S0163-1829(97)06236-X]

I. INTRODUCTION

$Al_xGa_{1-x}Sb$ mixed crystals have recently attracted a lot of interest as constituents in III-V semiconductor heterostructures with gap and band offset engineered to be used in advanced optoelectronic devices for near and medium infrared.[1] In particular, $Al_xGa_{1-x}Sb$-GaSb based double-heterostructure lasers operating at a wavelength of 1.78 μm and multiple-quantum-well (MQW) lasers at 1.646 μm have been reported.[2,3] Moreover, good response in the 8–14-μm range has been obtained in normal-incidence detectors and surface-emitting second-harmonic generators based on intersubband transitions in $GaSb/Al_xGa_{1-x}Sb$ MQW's.[4,5]

Despite this increasing interest, very little is known yet of the phonons of the $Al_xGa_{1-x}Sb$ alloys, which, like other III-V mixed crystals, show a two-mode behavior with regard to lattice vibrations in the long-wavelength limit ($q \approx 0$). Indeed, two optical phonon frequencies are observed to occur close to those of the end parents, GaSb and AlSb, with the strength of each mode dependent on the fraction x and $(1-x)$ of each component. This behavior has been discussed extensively.[6]

The most complete study of phonons in $Al_xGa_{1-x}Sb$, confirming the two-mode behavior, was made by Lucovsky *et al.*[7] who measured far-infrared (FIR) reflectance of layers grown by liquid-phase epitaxy (LPE) with $0 \leqslant x \leqslant 1$. First-order Raman-scattering (RS) spectra were measured by Biryulin *et al.*[8] on LPE layers; second-order RS on Bridgman-grown polycrystalline samples by Charfi *et al.*;[9] and first- and second-order RS on high-quality bulk crystal, only for $x = 0.14$, by Cuscó *et al.*[10] We determined the optical functions from 0.01 to 6 eV by reflectance and ellipsometry on layers with $0 \leqslant x \leqslant 0.5$, grown by molecular-beam epitaxy (MBE).[11] $Al_xGa_{1-x}Sb$ phonons have been studied theoretically in Refs. 12 and 13.

In the aforementioned studies the samples used differ in the quality, the surface, and the composition of the crystals, thus making a comparison of the experimental data difficult to obtain. For these reasons we undertook a systematic study of optical phonons in $Al_xGa_{1-x}Sb$ using the same samples for both Fourier-transform infrared (FTIR) reflectance and first- and second-order RS measurements, which supply complementary information.

Samples with $0 \leqslant x \leqslant 0.5$ (the most used compositions in optoelectronic devices) were grown by (MBE) and well characterized to assure good structural, compositional and optical quality. Fitting of the experimental spectra with the harmonic oscillators was also performed to obtain the transverse-optical (TO) and longitudinal-optical (LO) mode frequencies, the damping constants, and the oscillator strengths. These quantities play an important role not only in the analysis and intepretation of the vibrational spectra, but also in optical applications and diagnostics.

II. EXPERIMENT

The $Al_xGa_{1-x}Sb$ layers were prepared by MBE in an Intevac Gen II modular growth chamber on (100)-GaSb substrates. The Al mole fraction x in the alloys was between 0.0 and 0.5 with steps of 0.1. The compositions were measured by reflection high-energy electron diffraction oscillations and were accurate to within $\pm 5\%$. The layers were grown either directly on the substrates or on 1–5-μm-thick GaSb buffer layers. The nominal layer thicknesses were 1 μm for $x = 0.1$, 0.3, and 0.5, 4 μm for $x = 0.2$, and 3 μm for $x = 0.4$; the real thicknesses were determined from interference fringes in the subgap region. The $Al_{0.5}Ga_{0.5}Sb$ layers had 5-nm GaSb cap

layers to protect the reactive $Al_xGa_{1-x}Sb$ material. In order to improve the homogeneity and the purity of the material, we avoided In bonding of substrates by radiatively heating them; the growth temperature T_s was monitored with an optical pyrometer. T_s and the $Sb_4/(Al+Ga)$ beam equivalent pressure ratios (BEPR) were chosen to optimize the low-temperature photoluminescence features of $Al_xGa_{1-x}Sb$ and varied in the ranges 500 °C $\leqslant T_s \leqslant$ 600 °C and 5 $\leqslant$ BEPR $\leqslant$ 8. T_s increased with x and the highest value of BEPR was used for $x=0.2$. The GaSb film was grown at 450 °C with BEPRs of 7.[14]

Spectroscopic measurements were made on the MBE as-grown surface for all the samples, including the GaSb buffer layer. Room-temperature reflectance at near-normal incidence was measured in the wave number range 20–5000 cm^{-1} with a Bruker IFS 113v spectrometer, at a spectral resolution of 0.5 cm^{-1} from 20 to 600 cm^{-1} (FIR) and 4 cm^{-1} from 600 to 5000 cm^{-1} (MIR). A liquid-He-temperature-cooled Si bolometer and a deuterated triglycerine sulphite (DTGS) pyroelectric were used as detectors in FIR and MIR, respectively. A gold mirror was used as reference. The accuracy in the wave-number calibration was 0.001 cm^{-1} and the absolute reflectance was accurate to ± 0.005.

Raman spectra were measured by a Dilor LabRam spectroscopy system equipped with a HeNe laser and an air-Peltier-cooled charge-coupled detector. The laser was operating at a wavelength of 632.8 nm in the light-stabilizing mode and the incident power on the sample was kept at about 15 mW. The light beam was focused on the sample in a 1-μm-diameter spot in backscattering geometry. The spectra were recorded in the 100–1200-cm^{-1} spectral range, with a resolution of 1 cm^{-1} and additional improvement of signal-to-noise ratio was obtained by collecting several spectra over the same interval.

III. RESULTS AND DISCUSSION

The FIR reflectance spectra of the six samples are shown in Fig. 1, where the spectrum of a 1-μm-thick AlSb layer on a GaSb substrate, synthesized by assuming the data of Ref. 7, was also included for comparison. We noted that in the restrahlen region the spectrum of the GaSb MBE film practically coincided with that of the GaSb bulk sample. The alloy samples all display two main bands, one near 220 cm^{-1} and the other near 320 cm^{-1}, which are typical of two-mode systems: they can be characterized as GaSb-like and AlSb-like, respectively, because of their obvious relationship to the reststrahlen bands of GaSb and AlSb, due to IR-active TO phonons.

Amplitude, position, and shape of the FIR bands depend not only on the Al content (x) but also on the layer thickness. For the thinnest layers (corresponding to $x = 0.1$, 0.3, and 0.5) the GaSb-like structure of the alloy appears as a shoulder on the low-energy side of the reflectance peak of the GaSb bulk (buffer and substrate): this shoulder decreases in amplitude and redshifts as x increases, while the restrahlen band of GaSb bulk maintains constant intensity, position, and dispersionlike shape. Correspondingly, the AlSb-like band increases in strength and shifts toward higher frequencies and its minimum is quenched. On the other hand,

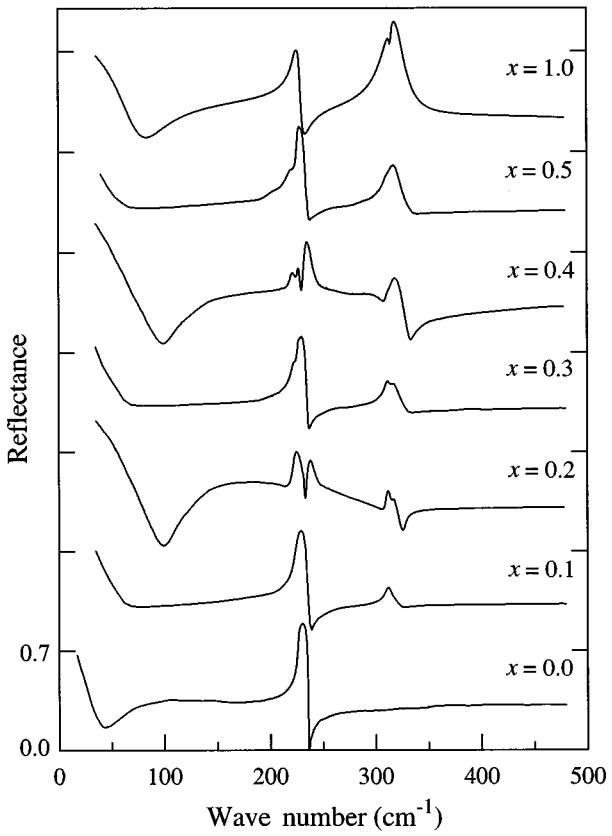

FIG. 1. FIR reflectance of $Al_xGa_{1-x}Sb$ MBE layers on GaSb with different x values. Each spectrum is displaced vertically by 0.7 to facilitate viewing. The spectrum of AlSb ($x = 1.0$) on GaSb substrate is calculated assuming the data of Ref. 7.

for the thickest layers ($x = 0.2$ and 0.4) the GaSb-like structure displays some oscillations while the AlSb-like structure has a dispersive shape. All the aforementioned features can be ascribed to interference effects, strongly dependent on the layer thickness and due to multireflection at the interfaces between the $Al_xGa_{1-x}Sb$ layer and the air or the substrate. Moreover, the high background hole concentration ($p \cong 10^{17}$ cm^{-3}, due to native complex defects of the GaSb-bulk substrate)[15] and the far lower number of free carriers in the buffer and alloy layers, determine the high reflectance tail and the free-carrier plasma minimum below the restrahlen region.

The interference effects, also appearing in the simulated spectrum for $x = 1$, can be well reproduced in the fit procedure thus providing additional evidence of the good interface quality and the uniformity of the thickness.

In order to obtain the phonon-mode parameters directly, the experimental spectra were fitted with the reflectance expression of a three-phase system (air, $Al_xGa_{1-x}Sb$ layer, GaSb buffer and substrate). The complex dielectric function $\tilde{\epsilon}(\nu)=\epsilon_1(\nu)+i\epsilon_2(\nu)$ of the alloy was constructed, for each x, as a superposition of two damped harmonic oscillators[7] corresponding to the GaSb- and AlSb-like plasmon modes. Hence,

$$\tilde{\epsilon}(\nu)=\epsilon_\infty+\sum_{j=1}^{2}\frac{S_j}{\nu_j^2-\nu^2+i\gamma_j\nu}, \qquad (1)$$

TABLE I. Harmonic oscillator parameters of the best fit to the reflectance spectra of $Al_xGa_{1-x}Sb$ layers on GaSb. The values obtained from Raman spectra are also reported (italic). The parameters of AlSb ($x = 1.0$) are from Refs. 7 and 8.

$Al_xGa_{1-x}Sb$		GaSb-like mode				AlSb-like mode			
x	ε_∞	ν_{TO} (cm^{-1})	ν_{LO} (cm^{-1})	S (10^4 cm^{-2})	γ (cm^{-1})	ν_{TO} (cm^{-1})	ν_{LO} (cm^{-1})	S (10^4 cm^{-2})	γ (cm^{-1})
0.0	14.50	227.1	235.8	5.57	0.95				
		227.2	*234.3*						
0.1	14.04	225.1	232.1	4.53	3.09	314.0	316.4	2.17	8.50
		225.4	*233.7*			*314.3*	*318.0*		
0.2	13.58	224.1	230.6	4.00	4.50	315.3	318.9	3.11	8.40
		223.9	*230.8*			*313.9*	*320.0*		
0.3	13.12	223.0	228.8	3.53	5.54	316.2	321.0	4.04	8.30
		221.6	*228.7*			*314.4*	*322.5*		
0.4	12.66	220.7	226.1	3.09	6.30	317.1	324.1	5.71	8.10
		219.2	*225.2*			*315.3*	*325.0*		
0.5	12.20	218.8	224.0	2.84	6.56	*317.7*	*327.1*	7.40	7.21
		217.3	*222.7*			*316.1*	327.9		
1.0	9.88 [a]					318.8[a]	339.5[a]	13.50[a]	1.88[a]
						319.9[b]	*340.0*[b]		

[a]Reference 7.
[b]Reference 8.

where ϵ_∞, ν_j, S_j, and γ_j, which are also the free parameters of the fit, represent, in order, the high-frequency dielectric constant, the oscillator frequency (corresponding to the TO phonon), the oscillator strength, and the phenomenological damping. The least-square fit was carried out using the CERN library MINUIT program, based on the Metropolis algorithm; the resulting standard deviation was $\sigma \leqslant 2 \times 10^{-2}$ for all the spectra. The best-fit parameters are reported in Table I and deserve some comment and comparison with those obtained by Lucovsky *et al.*[7] from FIR reflectance on LPE layers.

(i) ϵ_∞ values vary linearly between the extreme values of 14.5 for GaSb and 9.88 for AlSb, and for $x \leqslant 0.5$ are systematically 0.2 higher than those reported in Ref. 7. This small discrepancy can be attributed both to the absolute R values and to the fitted spectral range. The ϵ_∞ values were consistent with the dielectric response at higher frequencies determined by reflectance, transmittance, and ellipsometry on the same samples.[11] For the GaSb MBE sample $\epsilon_\infty = 14.5$ is in good agreement with the value of 14.44 quoted in Ref. 16 for a bulk crystal, and gives a static dielectric constant $\epsilon_0 = \epsilon_\infty(\nu_{LO}/\nu_{TO})^2 = 15.7$.

(ii) The LO frequency was derived from the maximum in the energy-loss function $-\mathrm{Im}(1/\tilde{\epsilon})$, i.e., $\nu_{LO}^2 = S/\epsilon_\infty + \nu_{TO}^2$. Both ν_{TO} and ν_{LO} for the GaSb-like mode, as well as the oscillator strengths, systematically decrease as the volume fraction of GaSb in the alloy decreases, i.e., with increasing x. The same occurs for the AlSb-like mode with decreasing x. By extrapolating the GaSb-like (AlSb-like) branches to $x = 1$ ($x = 0$), the TO-LO splitting is reduced to zero, in correspondence with the frequency of the local vibrational mode of Ga in AlSb (Al in GaSb). This behavior was predicted in the theoretical models of Refs. 12 and 13, and agrees with the results in Refs. 7 and 8.

(iii) The damping constants γ of the alloys are substantially larger than those of the binary parents. In particular, the damping of the GaSb-like band increases and that of the AlSb-like mode decreases with increasing x. This behavior—observed in other mixed crystals[6]—has to be ascribed to the relative content of each cation in the alloys and reflects the different order of each sublattice. We note that both γ_j and S_j differ up to a maximum of 10% from those reported in Ref. 7.

Figure 2 shows the room-temperature Raman spectra (RS) of the GaSb (bulk and MBE layer) and $Al_{0.1}Ga_{0.9}Sb$ samples in detail, with the assignment of the main structures at the different symmetry points of the Brillouin zone.[9,10,17] The notation is standard: T, L, A, and O indicate transverse, longitudinal, acoustic, and optic modes, respectively; the subscripts g and a indicate GaSb- and AlSb-like modes in the alloy, respectively.

Concerning the GaSb spectra [Fig. 2(a)] the first thing we noticed was that the GaSb MBE layer and the GaSb bulk give quasicoincident spectra, thus confirming the results of FTIR reflectance. The main peak, at ~ 234 cm^{-1}, is due to the LO mode, while the shoulder on its low-energy side corresponds to the TO mode. The appearance of the TO phonon, though forbidden in the backscattering configuration on a (100) face, was already evidenced both in GaSb as well as in other (AlGa)(AsSb) systems.[19,20] The mechanism for this selection rule violation is not clear. The less intense and structured bands on both sides of the dominant first-order modes are due to the second-order Raman modes. We attributed them to overtones and combinations at specific symmetry points following the conclusions in previous experimental and theoretical works,[9,13,17] which were also based on neutron scattering data. In particular the lowest frequency band (100–180 cm^{-1}) is attributable to acoustic phonon combinations; the intermediate band (250–300 cm^{-1}) to both acoustic and optic phonons, and the highest band (420–470 cm^{-1}) to optic overtones.

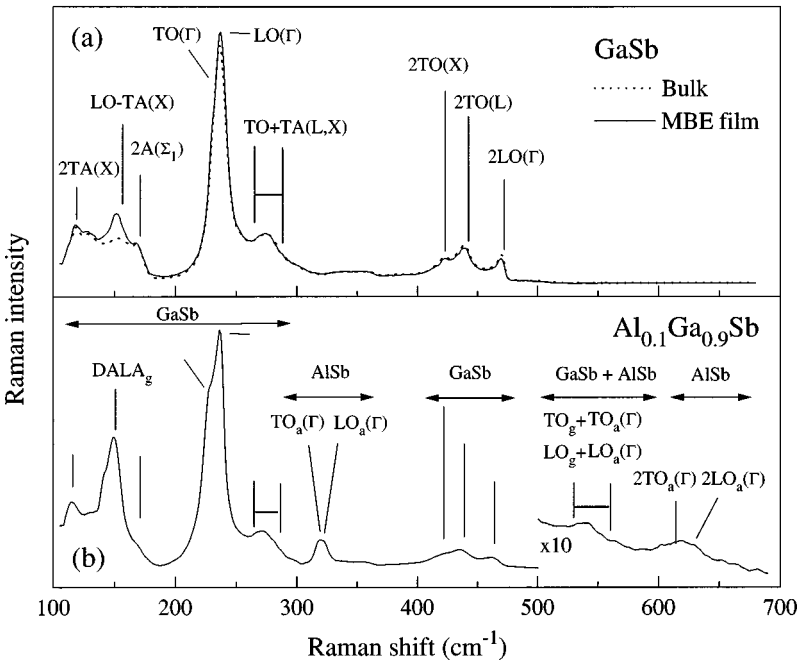

FIG. 2. First- and second-order Raman spectra of (a) GaSb (bulk and MBE film) and (b) $Al_{0.1}Ga_{0.9}Sb$ MBE layer on GaSb. The main structures are assigned in detail, based on Refs. 9, 10, and 17. In (b) lines without script refer to the analogous GaSb-like modes attributed in (a). For the notation see text.

The Raman spectrum of $Al_{0.1}Ga_{0.9}Sb$ in Fig. 2(b) strongly resembles that of GaSb, but a new clear band appears around 325 cm^{-1}, in correspondence with the AlSb-like TO and LO phonons, which in pure AlSb fall at 319 and 340 cm^{-1}, respectively.[18] The very weak band between 500 and 550 cm^{-1} can be attributed to the combination of GaSb-like and AlSb-like optic modes, while the still weaker band at $\sim$ 620 cm^{-1} is due to the overtones of AlSb-like TO and LO modes. Moreover the peak at $\sim$ 150 cm^{-1}, which increases with x and is also observed in $Al_xGa_{1-x}As$ alloys,[19] has been explained as a disorder-activated longitudinal acoustic (DALA) mode, resulting from the relaxation of the selection rules in the alloy samples.[10,19]

The RS spectra of all the samples are displayed in Fig. 3. As x increases the first-order GaSb-like band redshifts and lowers, while the AlSb-like band blueshifts and rises; the other two-phonon structures, except for the DALA modes, disappear progressively.

In order to obtain the values of ν_{TO} and ν_{LO} phonon frequencies, each GaSb- and AlSb-like first-order structure was fitted with two Lorentzian line shapes. The least-square fit ($\sigma \leqslant 10^{-2}$) yielded the values reported in Table I with a confidence interval of $\pm$ 2 cm^{-1}.

The compositional dispersion of TO and LO phonon frequencies is better shown in Fig. 4, where the curves obtained in Ref. 7 by fitting FIR reflectance data with a quadratic polynomial in x are also reported. From the examination of Table I and Fig. 4 some general remarks can be inferred.

(i) The TO frequencies obtained from FTIR reflectance coincide with those from Ref. 7 on LPE films within their declared experimental uncertainty ($\pm$ 0.5 cm^{-1}), apart from a systematic shift of $\sim$ 1 cm^{-1}, probably due to the different accuracy in the wave-number calibration (nominally 0.001 cm^{-1} of our FTIR spectrometer versus 0.5 cm^{-1} of their dispersive instrument).

(ii) The TO and LO frequencies derived from FTIR and RS differ by up to 1.6 cm^{-1}; however, for the AlSb-like modes the deconvolution of the experimental RS structure and thus the RS fit values are rather uncertain.

(iii) The dependence of phonon frequencies on x and the LO-TO splittings have been analyzed in different theoretical models.[7,8,12,13] Nevertheless, the best fit between theory and experiment was obtained in Ref. 7 by using a modified

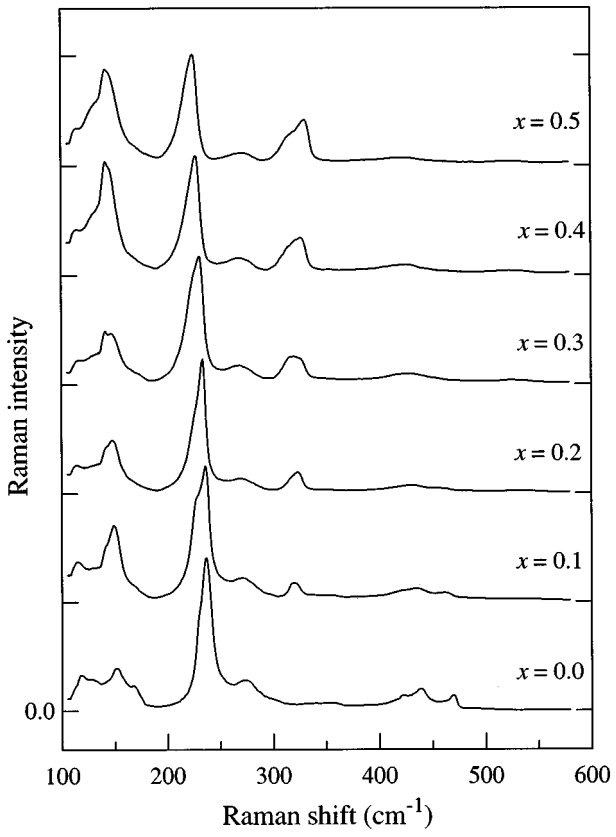

FIG. 3. First- and second-order Raman spectra of $Al_xGa_{1-x}Sb$ MBE layers on GaSb with different x values. Each spectrum is displaced vertically to facilitate viewing.

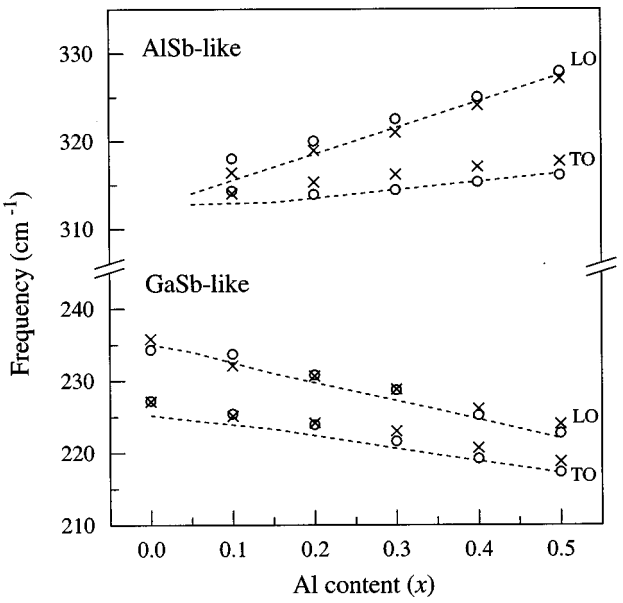

FIG. 4. Frequencies of GaSb- and AlSb-like TO(Γ) and LO(Γ) modes obtained from FTIR (crosses) and *RS* (open circles) of $Al_xGa_{1-x}Sb$ MBE layers on GaSb. The interpolations of the reflectance results of Ref. 7 are also reported (dashed lines).

random-element-isodisplacement model, which allows a different compositional variation of both the force constants and their derivatives with respect to x, through six free parameters.

IV. CONCLUSIONS

A series of thin layers of $Al_xGa_{1-x}Sb$ with $0.0 \leqslant x \leqslant 0.5$ was grown on a GaSb substrate by MBE. The samples were well characterized in their microstructural composition and optical quality.

FIR reflectance and Raman spectra, systematically and carefully measured, confirmed the two-mode behavior of lattice vibrations for all compositions. The analysis of the results from *R* spectra yielded TO and LO phonon frequencies that agreed very well, within the experimental error, with those from Raman scattering and those deduced from *R* measurements on thicker LPE layers. In particular, the GaSb epitaxial film gives an optical response identical to that of the bulk crystal.

Disorder in the cation sublattices of the alloys causes TO and LO line broadenings to be larger than those in pure binary compounds, and partially relaxes the selection rules in two-phonon Raman scattering.

The TO and LO phonon frequencies of each binarylike mode redshift and their splitting decreases as the volume fraction of the corresponding binary constituent in the alloy decreases. This behavior agrees with the results derived from different theoretical models.

ACKNOWLEDGMENTS

The authors wish to thank Dr. P. Valisa (Instruments S.A. Italy) for his assistance in doing Raman measurements.

[1] For a recent review, see A. G. Milnes and A. Y. Polyakov, Solid-State Electron. **36**, 806 (1993).
[2] W. T. Tsang and N. A. Olsson, Appl. Phys. Lett. **43**, 8 (1993).
[3] Y. Ohmori, S. Tarucha, Y. Horikoshi, and H. Okamoto, J. Phys. Soc. Jpn. **23**, L94 (1984).
[4] H. Xie and W. I. Wang, Appl. Phys. Lett. **63**, 796 (1993); H. Xie, W. I. Wang, L. R. Meyer, and J. R. Ram-Mohan, *ibid.* **65**, 2048 (1994).
[5] D. Y. Zhang, N. Baruch, and W. I. Wang, Appl. Phys. Lett. **63**, 1068 (1993).
[6] D.W. Taylor, in *Optical Properties of Mixed Crystals*, edited by R. J. Elliot and I. P. Ipatova (North-Holland, Amsterdam, 1988).
[7] G. Lucovsky, K. Y. Cheng, and G. L. Pearson, Phys. Rev. B **12**, 4135 (1975).
[8] Yu F. Biryulin, G. M. Zinger, I. P. Ipatova, Yu E. Pozhidaev, and Yu V. Shmartsev, Fiz. Tekh. Poluprovodn. **13**, 1628 (1979) [Sov. Phys. Semicond. **13**, 948 (1979)].
[9] F. Charfi, M. Zouaghi, A. Joullie, M. Balkanski, and Ch. Hirlimann, J. Phys. (Paris) **41**, 83 (1980).
[10] R. Cuscó, L. Artus, and K. W. Benz, J. Phys. Condens. Matter **7**, 7069 (1995).
[11] R. Ferrini, M. Galli, G. Guizzetti, M. Patrini, A. Bosacchi, and S. Franchi, *The Physics of Semiconductors: Proceedings of the XXIII International Conference*, edited by M. Scheffler and R. Zimmermann (World Scientific, Singapore, 1996), p. 265.
[12] G. Ahuja, H. C. Gupta, and L. M. Tawari, Physica (Amsterdam) **124B**, 225 (1984).
[13] D. N. Talwar, M. Vandevyver, and M. Zigone, Phys. Rev. B **23**, 1743 (1981).
[14] A. Bosacchi, S. Franchi, P. Allegri, V. Avanzini, A. Baraldi, C. Ghezzi, R. Magnanini, A. Parisini, and L. Tarricone, J. Cryst. Growth **150**, 844 (1995).
[15] S. C. Chen and Y. K. Su, J. Appl. Phys. **66**, 350 (1989).
[16] M. Hass and B. W. Henvis, J. Phys. Chem. Solids **23**, 1099 (1962).
[17] P. B. Klein and R. K. Chang, Phys. Rev. B **14**, 2498 (1976).
[18] W. J. Turner and W. E. Reese, Phys. Rev. **127**, 126 (1972).
[19] O. K. Kim and W. G. Spitzer, J. Appl. Phys. **50**, 4362 (1979).
[20] P. V. Santos, A. K. Sood, M. Cardona, K. Ploog, Y. Ohmori, and H. Okamoto, Phys. Rev. B **37**, 6381 (1988).